Probing the Electronic Structure of [2Fe-2S] Clusters with Three Coordinate Iron Sites by Use of Photoelectron Spectroscopy

You-Jun Fu, Xin Yang, Xue-Bin Wang, and Lai-Sheng Wang*

Department of Physics, Washington State University, 2710 University Drive, Richland, Washington 99352, and W. R. Wiley Environmental Molecular Sciences Laboratory, Pacific Northwest National Laboratory, P.O. Box 999, Richland, Washington 99352

Received: October 22, 2004; In Final Form: December 6, 2004

Five series of [2Fe-2S] complexes, $[Fe_2S_2Cl_{2-x}(CN)_x]^-$, $[Fe_2S_2(SEt)_{2-x}Cl_x]^-$, $[Fe_2S_2(SEt)_{2-x}(CN)_x]^-$, $[Fe_2S_2Cl_{2-x}(OAc)_x]^-$ (OAc = acetate), and $[Fe_2S_2(SEt)_{2-x}(OPr)_x]^-$ (OPr = propionate) ($x = 0-2$), were produced by collision-induced dissociation of the corresponding [4Fe-4S] complexes, and their electronic structures were studied by photoelectron spectroscopy. All the [2Fe-2S] complexes contain a $[Fe_2S_2]^+$ core similar to that in reduced [2Fe] ferredoxins but with different coordination geometries. For the first three series, which only involve tricoordinated Fe sites, a linear relationship between the measured binding energies and the substitution number (x) was observed, revealing the independent ligand contributions to the total electron binding energies. The effect of the ligand increases in the order SEt → Cl → CN, conforming to their electron-withdrawing ability in the same order. The carboxylate ligands in the $[Fe_2S_2Cl_{2-x}(OAc)_x]^-$ and $[Fe_2S_2(SEt)_{2-x}(OPr)_x]^-$ complexes were observed to act as bidentate ligands, giving rise to tetracoordinated iron sites. This is different from their monodentate coordination behavior in the [4Fe-4S] cubane complexes, reflecting the high reactivity of the unsatisfied three-coordinate iron site in the [2Fe-2S] complexes. The [2Fe-2S] complexes with tetracoordinated iron sites exhibit lower electron binding energies, that is, higher reductive activity than the all tricoordinate planar clusters. The electronic structures of all the [2Fe-2S] complexes were shown to conform to the "inverted energy level scheme".

1. Introduction

Iron−sulfur clusters are common metallocenters in a wide variety of proteins and enzymes. To understand the properties and functionalities of Fe−S proteins, it is important to understand the electronic structure of the Fe−S cluster cores. The most extensively studied Fe−S active centers include mononuclear [1Fe] clusters in rubredoxins, [2Fe-2S] clusters in ferredoxins, and [4Fe-4S] clusters in ferredoxins and high-potential iron protein (HiPIP).[1−3] All of these clusters typically have tetrahedral coordination geometry at the Fe sites. On the other hand, tricoordinate Fe sites may play important roles in the active center of nitrogenase, the iron−molybdenum cofactor (FeMoco).[4−11] According to the original structural determination, FeMoco consisted of an $MoFe_7S_9$ cluster.[4−6] Six of the seven iron atoms in the cluster core possessed the rare distorted trigonal geometry, forming an approximate trigonal prism. The existence of an internal ligand atom X (X = C, N, or O) in the center of the FeMoco was recently discovered.[7] However, because the interaction between X and the surrounding six iron atoms is not strong and X is hypervalent, the Fe−X bonds are most likely disrupted during catalysis. Therefore, three-coordinate iron complexes are perhaps still reasonable candidates to mimic the possible reactive forms of FeMoco.[12,13] The electronic structure of the few reported synthetic three-coordinate iron complexes[12−16] all exhibits characteristics of antiferromagnetic interactions between the two iron sites,[12−14] similar to that of the [2Fe-2S] clusters with tetracoordination found in either ferredoxins or analogue complexes.[14−28] Density functional theory (DFT) calculations have been one of the major theoretical methods used to study the electronic structures of Fe−S proteins and analogues.[29−32] The calculations are consistent with both electron spin resonance (ESR) and Mossbauer experiments[14−28] and showed that the electronic structure of the [2Fe-2S] clusters conforms to the so-called "inverted level scheme", in which the energy levels of the ligand orbitals fall in the gap between the minority and majority spin states of the Fe 3d orbitals.[29−32]

We are interested in using photoelectron spectroscopy (PES) to investigate the electronic structures of Fe−S clusters in the gas phase.[33−41] PES gives direct energy level information and has the advantage that in the gas phase mass selection techniques allow species-specific information to be obtained from an equilibrium of different complexes in solution. Combining with bioinorganic structure design and synthesis, we have been able to perform systematic studies on ligand-free clusters,[33,38] clusters with small molecule ligands (both organic and inorganic),[34−39] and H-bonding effects.[41] We have confirmed the validity of the "inverted energy scheme" for ligand free clusters Fe_nS_m,[38] mononuclear complexes $[FeX_3]^-$ and $[FeX_4]^-$ (analogues of rubredoxin active center),[34−36] and tetranuclear complexes.[37−40] For the [4Fe] cubane complexes, we observed that the terminal ligands do not significantly perturb the electronic structure of the cubane, but they significantly change the electron binding energies, that is, the intrinsic redox potentials of the cubane.[37,39] Most interestingly, symmetric fissions of the doubly charged $[Fe_4S_4L_4]^{2-}$ cubane complexes into two identical $[Fe_2S_2L_2]^-$ clusters have been observed.[40] This finding provides the opportunity to access dinuclear Fe−S clusters with novel

* To whom correspondence should be addressed: e-mail ls.wang@pnl.gov.

10.1021/jp045177k CCC: $30.25
Published on Web 02/10/2005

coordination, which would have been difficult to synthesize in solution.

Here we present a PES study on several series of [2Fe-2S] clusters with tri- and tetracoordinated Fe−S sites, produced by symmetric fission of $[Fe_4S_4L_4]^{2-}$ complexes, to explore the influence of ligand and coordination geometry on their electronic structures and redox properties.

2. Experimental Methods

2.1. Sample Preparation. All sample preparations were carried out in a dry N_2 glovebox with O_2-free acetonitrile as solvent. Solutions (1×10^{-3} mol/L) of $[Fe_4S_4Cl_4]^{2-}$ (**1**) and $[Fe_4S_4(SEt)_4]^{2-}$ (-SEt = -SC_2H_5) (**2**) were prepared from (t-$Bu_4N)_2[Fe_4S_4Cl_4]$ and (t-$Bu_4N)_2[Fe_4S_4(SEt)_4]$ solid samples. Solution samples of $[Fe_4S_4Cl_{4-x}(CN)_x]^{2-}$ and $[Fe_4S_4Cl_{4-x}(OAc)_x]^{2-}$ (OAc = acetate) were prepared by mixing **1** with varying equivalents of (t-Bu_4N)CN and acetic acid. Solutions of $[Fe_4S_4(SEt)_{4-x}(CN)_x]^{2-}$ and $[Fe_4S_4(SEt)_{4-x}(OPr)_x]^{2-}$ (OPr = propionate) were prepared by mixing **2** with different equivalents of (t-Bu_4N)CN and propionic acid.[39] The concentration of the second ligand was tuned to optimize the abundance of a given dianionic species as the precursor for collision-induced dissociation (CID) experiments to produce the relevant [2Fe-2S] fission products. Solutions of $[Fe_4S_4Cl_{4-x}(SEt)_x]^{2-}$ were obtained by simply mixing solutions **1** and **2**. Singly charged anions with two identical terminal ligands, $[Fe_2S_2L_2]^-$ (L = Cl, SEt, CN, OAc, and OPr), were obtained by CID of $[Fe_4S_4L_4]^{2-}$, while $[Fe_2S_2LL']^-$ with two different terminal ligands were obtained by CID of $[Fe_4S_4L_2L'_2]^{2-}$.[40,41]

2.2. Electrospray Photoelectron Spectroscopy. The experiments were carried out with a PES apparatus equipped with an electrospray ionization (ESI) source, a time-of-flight (TOF) mass spectrometer, and a magnetic-bottle TOF photoelectron analyzer.[42] The precursor dianions $[Fe_4S_4L_4]^{2-}$ and $[Fe_4S_4L_2L'_2]^{2-}$ were produced by spraying the sample solutions through a 0.01 mm diameter syringe needle (biased at −2.2 kV) under N_2 atmosphere.[37] CID experiments were carried out by applying a voltage of 2.5−6.0 V to the first skimmer of the instrument.[40a,40b,42] All the anions were guided by a radio frequency quadruple ion guide into a 3D quadruple ion trap, where they were accumulated for 0.1 s and then were pulsed into the extraction zone of a TOF mass spectrometer. The species of interest were selected by a mass gate and decelerated before being intercepted by a probing laser beam in the photodetachment zone of the magnetic-bottle photoelectron analyzer. In the present study, we used three detachment photon energies, 157 nm (7.866 eV), 193 nm (6.424 eV) from an excimer laser, and 266 nm (4.661 eV) from a Nd:YAG laser. All experiments were performed at 20 Hz repetition rate with the ion beam off at alternating laser shots for background subtraction. Photoelectrons were collected at nearly 100% efficiency by the magnetic bottle and analyzed in a 4-m long electron flight tube. Photoelectron TOF spectra were collected and then converted to kinetic energy spectra, calibrated by the known spectra of I^- and O^-. The electron binding energy spectra presented here were obtained by subtracting the kinetic energy spectra from the detachment photon energies. The energy resolution ($\Delta E/E$) was about 2% as measured from the spectrum of I^- at 355 nm.

Due to the lack of vibrational resolution, the adiabatic detachment energies (ADEs) were measured by drawing a straight line along the leading edge of the threshold band and then adding a constant to the intersection with the binding energy axis to take into account for the instrumental resolution. The vertical detachment energies (VDEs) were measured from the PES peak maxima. Listed in Table 1 are the ADEs for the first PES peak and VDEs for both the first and second PES peaks for all the species from the respective 266 or 193 nm spectra.

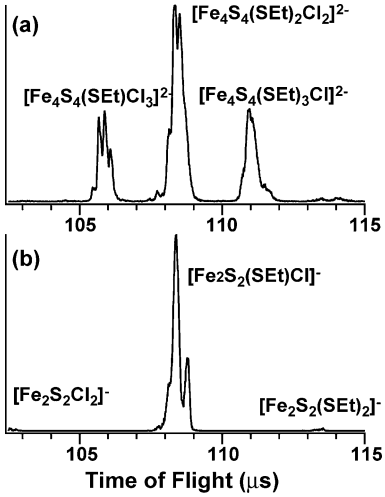

Figure 1. Electrospray mass spectra from a mixed solution of $[Fe_4S_4(SEt)_4]^{2-}$ and $[Fe_4S_4Cl_4]^{2-}$ in 1:1 molar ratio under (a) normal electrospray conditions and (b) collision-induced dissociation conditions.

3. Experimental Results

3.1. Collision-Induced Dissociation of $[Fe_4S_4(L_1)_{4-x}(L_2)_x]^{2-}$. Figure 1 shows the mass spectra obtained from a sample solution prepared by mixing solutions **1** and **2** at a 1:1 molar ratio. We observed three species under our normal ESI conditions (Figure 1a): $[Fe_4S_4(SEt)Cl_3]^{2-}$ at $m/z = 259$, $[Fe_4S_4(SEt)_2Cl_2]^{2-}$ at $m/z = 272$, and $[Fe_4S_4(SEt)_3Cl]^{2-}$ at $m/z = 285$. No parent dianion, $[Fe_4S_4Cl_4]^{2-}$ ($m/z = 246$), and only very weak $[Fe_4S_4(SEt)_4]^{2-}$ ($m/z = 298$) signals were present in the spectrum, indicating that at the 1:1 molar ratio in the original ESI solution the formation of mixed-ligand complexes was greatly favored. Under CID conditions (Figure 1b), only one dominant peak, $[Fe_2S_2(SEt)Cl]^-$ at $m/z = 272$, was observed at the same position as the parent, $[Fe_4S_4(SEt)_2Cl_2]^{2-}$. But the $[Fe_2S_2(SEt)Cl]^-$ daughter anions have a different isotope pattern. Figure 1b indicated that the fission processes in our ESI source under the CID conditions were rather complete with very little parent anions left. Similar mass spectra were obtained for other mixed-ligand systems.

3.2. PES Spectra at 193 nm. We were able to obtain the PES spectra of all five series of [2Fe-2S] complexes at 193 nm, as shown in Figure 2. The gradual spectral changes induced by the ligand substitution were revealed in each series.

3.2.1. $[Fe_2S_2Cl_{2-x}(CN)_x]^-$ ($x = 0-2$). The spectral patterns of these three species (Figure 2a) are similar to those of their cubane parents, $[Fe_4S_4Cl_4]^{2-}$, $[Fe_4S_4Cl_2(CN)_2]^{2-}$, and $[Fe_4S_4(CN)_4]^{2-}$.[39] The first two peaks (X and A) are well separated. The gaps between peaks X and A change with the CN^- substitution, increasing from 0.59 to 0.65 to 0.79 eV for $x = 0$, 1, and 2, respectively. This observation is different from the doubly charged cubane parents, where the separations between the first two similar spectral features were relatively constant with respect to the CN^- substitution.[39] The ADEs of the three species are 3.77, 4.01, and 4.32 eV, respectively, for $x = 0$, 1, and 2, due to the stronger electron-withdrawing capability of CN^- than Cl^-.

3.2.2. $[Fe_2S_2(SEt)_{2-x}(CN)_x]^-$ and $[Fe_2S_2(SEt)_{2-x}Cl_x]^-$ ($x = 0-2$). The PES spectra of these two series were also well-resolved, exhibiting similar spectral patterns to their respective

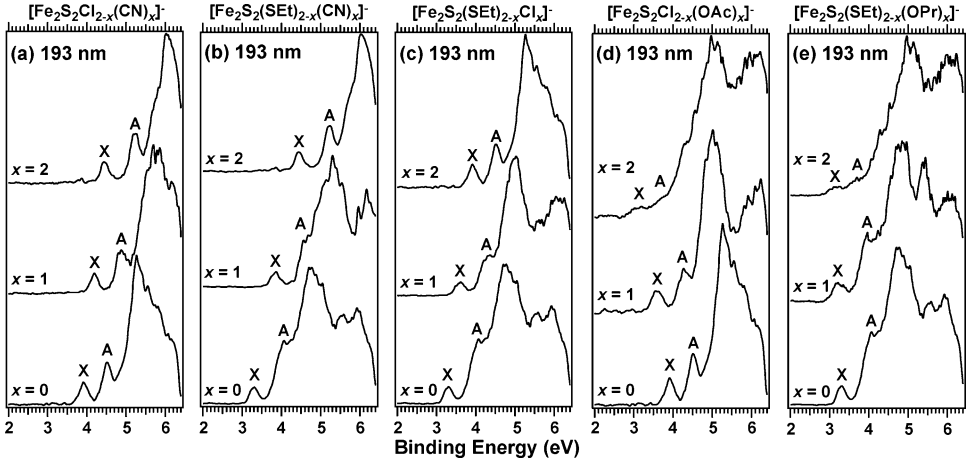

Figure 2. Photoelectron spectra at 193 nm (6.424 eV): (a) $[Fe_2S_2Cl_{2-x}(CN)_x]^{1-}$; (b) $[Fe_2S_2(SEt)_{2-x}(CN)_x]^{1-}$; (c) $[Fe_2S_2(SEt)_{2-x}Cl_x]^{1-}$; (d) $[Fe_2S_2(SEt)_{2-x}(OAc)_x]^{1-}$; (e) $[Fe_2S_2(SEt)_{2-x}(OPr)_x]^{1-}$.

cubane parents.[39] In the case of the $[Fe_2S_2(SEt)_{2-x}(CN)_x]^-$ series (Figure 2b), the second feature (A) for $x = 0$ and 1 was shown as shoulders. For this series, the X−A gap remains the same at about 0.76 eV in all three species. The ADEs of the three species were determined to be 3.17, 3.68, and 4.32 eV, with increasing CN^- substitution. The X−A gap for the $[Fe_2S_2(SEt)_{2-x}Cl_x]^-$ series decreases from 0.76 to 0.63 to 0.59 eV, but the ADEs increase from 3.17 to 3.46 to 3.77 eV, respectively, for $x = 0$, 1, and 2.

3.2.3. $[Fe_2S_2Cl_{2-x}(OAc)_x]^-$ and $[Fe_2S_2(SEt)_{2-x}(OPr)_x]^-$ ($x = 0-2$). It was surprising that the ADEs seemed to decrease with the OAc ligand substitution in the $[Fe_2S_2Cl_{2-x}(OAc)_x]^-$ series (Figure 2d), quite different from the above three series. For $x = 0$, 1, and 2, the ADEs decreased from 3.77 to 3.39 to 2.80 eV. Furthermore, the spectrum of $[Fe_2S_2(OAc)_2]^-$ appeared to be poorly resolved. The X and A bands became part of what seemed to be a long tail at the lower binding energy side. This series is clearly very different from the other [2Fe-2S] complexes and is also very different from the $[Fe_4S_4Cl_{4-n}(OAc)_n]^{2-}$ cubane parents, where the ADEs increase with increasing OAc substitution.[39] The PES spectral features of the OAc-substituted cubanes were also better resolved and were similar to the parent $[Fe_4S_4Cl_4]^{2-}$.

The PES spectra of $[Fe_2S_2Cl_{2-x}(OPr)_x]^-$ are shown in Figure 2e. With the substitution of SEt by OPr, the ADEs were also observed to decrease in the $[Fe_2S_2(SEt)_{2-x}(OPr)_x]^-$ series, similar to the $[Fe_4S_4Cl_{4-n}(OAc)_n]^{2-}$ series. $[Fe_2S_2(OPr)_2]^-$ gave an almost identical spectrum to that of $[Fe_2S_2(OAc)_2]^-$, suggesting that the additional CH_2 group in the -OPr ligand has no detectable influence on the redox properties of the [2Fe-2S] complexes.

3.3. PES Spectra at 157 nm. Figure 3 shows the 157-nm spectra of $[Fe_2S_2L_2]^-$ (L = SEt, Cl, CN) and two mixed-ligand species, $[Fe_2S_2Cl(CN)]^-$, $[Fe_2S_2Cl(OAc)]^-$. The 157-nm photons allowed a broad energy range to be observed. All the 157-nm spectra shown in Figure 3 exhibit similar spectral patterns in the low binding energy range with the two well-resolved bands, X and A, similar to the 193-nm data (Figure 2). In the high binding energy range, features from the terminal ligands, that is, SEt, Cl, CN, and OAc, were observed, which were similar to those observed in the cubane complexes,[39] though at much higher binding energies in the singly charged [2Fe-2S] complexes. In fact, the whole spectral patterns of the $[Fe_2S_2L_{2-x}L'_x]^-$ complexes revealed at 157 nm are very similar to those of their cubane parents, reflecting the similarity in their underlying electronic strucrures.[37,40a]

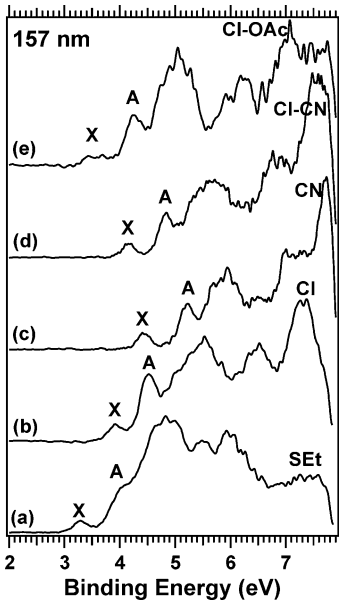

Figure 3. Photoelectron spectra at 157 nm (7.866 eV): (a) $[Fe_2S_2(SEt)_2]^-$; (b) $[Fe_2S_2Cl_2]^-$; (c) $[Fe_2S_2(CN)_2]^-$; (d) $[Fe_2S_2Cl(CN)]^-$; (e) $[Fe_2S_2Cl(OAc)]^-$.

3.4. PES Spectra at 266 nm. PES spectra for a selected set of [2Fe-2S] complexes were also taken at 266 nm, which gave better resolved spectra for the X band (Figure 4) and yielded more accurate ADEs and VDEs for these species (Table 1). Spectra at 266 nm were not able to be obtained for other [2Fe-2S] species, either due to their high binding energies or weak mass intensities.

4. Discussion

4.1. Influence of Terminal Ligands on the Intrinsic Redox Potentials of $[Fe_2S_2L_{2-x}L'_x]^-$. Photodetachment involves removal of electrons from occupied molecular orbitals. Thus, the ADE of the lowest binding energy peak (X) represents in fact the intrinsic oxidation energy of a [2Fe-2S] complex. In a recent study,[39] we observed a linear correlation between ADE and ligand substitution number for several series of cubane complexes, $[Fe_4S_4L_{4-x}L'_x]^{2-}$, indicating that each ligand contributes independently and additively to the redox potentials of the cubane complexes. This result also suggests that the [4Fe-4S] cubane core is a robust structural unit and that the core−ligand interactions are electrostatic in nature. This behavior is remi-

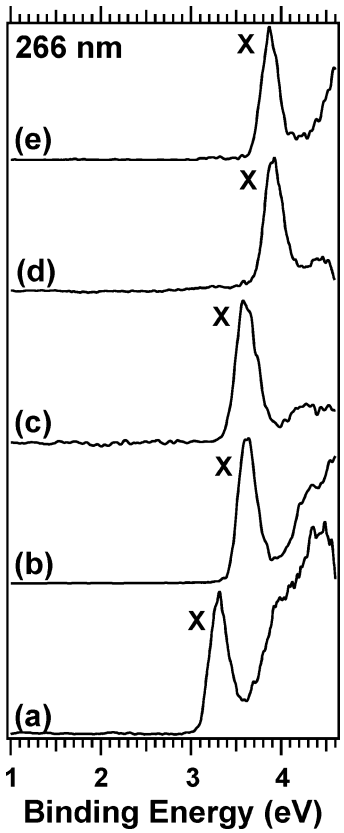

Figure 4. Photoelectron spectra at 266 nm (4.661 eV): (a) $[Fe_2S_2(SEt)_2]^-$; (b) $[Fe_2S_2(SEt)Cl]^-$; (c) $[Fe_2S_2Cl(OAc)]^-$; (d) $[Fe_2S_2Cl_2]^-$; (e) $[Fe_2S_2(SEt)(CN)]^-$.

TABLE 1: Adiabatic and Vertical Electron Binding Energies[a] of the $[Fe_2S_2L_2]^-$ and $[Fe_2S_2LL']^-$ Complexes

	ADE	VDE (X)	VDE (A)
$[Fe_2S_2Cl_2]^-$	3.77(6)	3.92(5)	4.51(5)
$Fe_2S_2(SEt)_2]^-$	3.17(6)	3.31(6)	4.07(6)
$[Fe_2S_2(SEt)Cl]^-$	3.46(5)	3.62(5)	4.35(10)
$[Fe_2S_2(SEt)(CN)]^-$	3.68(10)	3.87(8)	4.62(10)
$[Fe_2S_2Cl(OAc)]^-$	3.39(8)	3.56(6)	4.27((6)
$[Fe_2S_2(SEt)(OPr)]^-$	3.05(10)	3.22(12)	3.97(8)
$[Fe_2S_2(OPr)_2]^-$	2.84(13)	3.20(15)	3.70(15)
$[Fe_2S_2(OAc)_2]^-$	2.80(15)	3.20(15)	3.77(15)
$[Fe_2S_2Cl(CN)]^-$	4.01(6)	4.19(5)	4.84(10)
$[Fe_2S_2(CN)_2]^-$	4.32(6)	4.44(5)	5.23(6)

[a] Binding energies are given in electronvolts and were measured from the photoelectron spectra (Figures 2 and 4).

niscent of mononuclear transition metal complexes, where similar linear correlation was known for mixed-ligand species.[43−46] In the present work, we observed similar linear correlations for the three series of [2Fe-2S] complexes involving the SEt, Cl, and CN ligands, as displayed in Figure 5. Although there are only three points for each series, the linearity is obvious. Hence, we can conclude that these three ligands contribute to the redox properties of the [2Fe-2S] core independently and additively. Furthermore, we observed that the contributions to the binding energies increase for the three ligands in the order SEt < Cl < CN, consistent with their respective electron-withdrawing capabilities.[37,39]

4.2. Electronic Structure of the $[Fe_2S_2L_{2-x}L'_x]^-$ Clusters with Two Tricoordinated Iron Sites. According to broken symmetry DFT calculations,[29−32] strong spin polarization in Fe−S clusters would split the majority and minority spin states (up and down) of the 3d orbitals in each Fe site by 4−5 eV. In the oxidized state, the five d electrons in each ferric site of

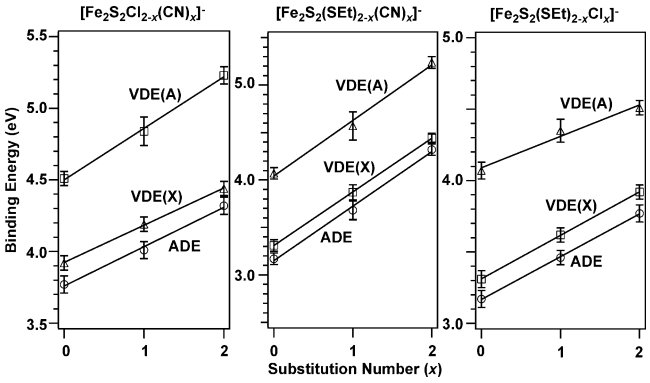

Figure 5. Linear correlation between electron binding energies and ligand substitution number x for (a) $[Fe_2S_2Cl_{2-x}(CN)_x]^{1-}$, (b) $[Fe_2S_2(SEt)_{2-x}(CN)_x]^{1-}$, and (c) $[Fe_2S_2(SEt)_{2-x}Cl_x]^{1-}$.

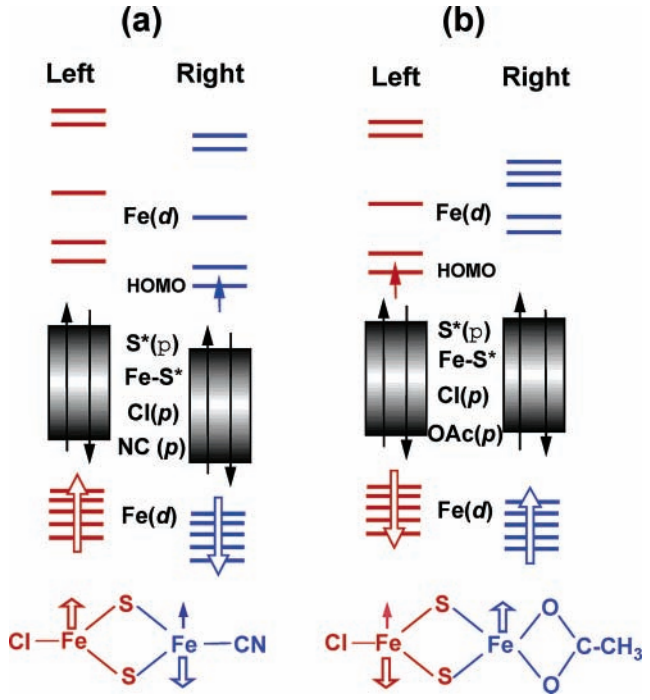

Figure 6. Schematic diagrams of the "inverted energy level scheme" of the [2Fe-2S] clusters with two different terminal ligands and their structures: (a) $[Fe_2S_2Cl(CN)]^-$; (b) $[Fe_2S_2Cl(OAc)]^-$.

$[Fe_2S_2]^{2+}$ would occupy the lower energy majority spin states to give two high-spin Fe sites. Antiferromagnetic coupling between the two Fe sites results in an overall low-spin cluster ($S = 0$). In the reduced state, the extra electron in $[Fe_2S_2]^+$ would occupy a minority spin level and localize on one of the two Fe sites, giving rise to an overall spin state of $S = {}^1/_2$. In the MO energy levels, the MOs dominated by the ligands fall in the gap between the minority and majority spin states of the d orbitals, resulting in the so-called "inverted level scheme". The validity of this model was proved by both ESR and Mossbauer experiments.[14−28] There is experimental evidence of two high-spin, antiferromagnetically coupled metal centers in tricoordinate transition metal complexes.[12,13,16] A recent DFT calculation yielded similar electronic structures for $[Fe_2S_2L_2]^-$ clusters with two tricoordinate iron sites.[40] Figure 6 shows the schematic diagram of the "inverted level scheme" of $[Fe_2S_2]^+$ for two different coordination geometries and will be used to understand the PES data.

Overall, the PES spectral patterns of $[Fe_2S_2L_{2-x}L'_x]^-$ (Figures 2−4) are similar to those observed for their doubly charged

parents, $[Fe_4S_4L_{4-x}L'_x]^{2-}$.[39] The relatively high binding energies and the absence of spectral cutoff in the higher binding energy side in the spectra of the $[Fe_2S_2L_{2-x}L'_x]^-$ species are consistent with their singly charged state, that is, the lack of intramolecular Coulomb repulsion and the repulsive Coulomb barrier present in their doubly charged parent anions.[39,47−51] The similarity between the overall spectral patterns of $[Fe_2S_2L_{2-x}L'_x]^-$ and $[Fe_4S_4L_{4-x}L'_x]^{2-}$ suggests that they follow the "inverted level schemes". This has been shown and proven previously in our studies involving fission of cubanes with four identical terminal ligands.[40] Figure 6a is a schematic diagram showing the inverted level scheme for tricoordinated [2Fe-2S] complexes with two different terminal ligands, $[Fe_2S_2LL']^-$. $[Fe_2S_2Cl(CN)]^-$ is used as an example in Figure 6a.

The PES features for the three series with Cl/CN, SEt/CN, and SEt/Cl ligands (Figure 2a−c) can all be qualitatively understood by use of Figure 6a. The first peak (X) should be due to detachment of the highest occupied molecular orbital (HOMO) electron, which is in the minority d spin state. The second peak (A) should correspond to HOMO − 1, which is mainly due to the bridging sulfide ligands. The intense and congested features beyond the A band in Figure 2a−c should correspond to MOs mainly composed of Fe−S and Fe−L(L′) bonding and nonbonding orbitals. At the very high electron binding energy side in the 157-nm spectra (∼7 eV), features due to the terminal ligand lone pairs appeared, as labeled in Figure 3. The slightly different X−A gaps in the PES spectra of the $[Fe_2S_2Cl_{2-x}(CN)_x]^-$ series (Figure 2a) indicate that the terminal ligands have some perturbation to the relative energy levels of HOMO and HOMO − 1, but the perturbation is not large enough to change the electronic structure of [2Fe-2S] complexes significantly.

For complexes with two identical terminal ligands, $[Fe_2S_2L_2]^-$, the minority spin electron can localize on either Fe site. But for complexes with two different terminal ligands, $[Fe_2S_2LL']^-$, the two Fe sites are nonequivalent. We expected that the extra spin would localize on the Fe site that is coordinated to a terminal ligand with stronger electron-withdrawing ability. For example, the mixed-ligand species, $[Fe_2S_2Cl(CN)]^-$, can be reformulated as $[Cl\text{-}Fe^{III}\text{-}S_2\text{-}Fe^{II}\text{-}CN]^-$ (Figure 6a) because CN is a stronger electron acceptor than Cl. Similar to the mixed-ligand cubane complexes, $[Fe_4S_4L_{4-x}L'_x]^{2-}$,[39] we observed a linear relationship between the binding energies and the substitution number (x), with the binding energy of $[Fe_2S_2LL']^-$ falling exactly between the values of $[Fe_2S_2L_2]^-$ and $[Fe_2S_2L'_2]^-$ (Figure 5). This observation implies that even though in the [2Fe-2S] core the minority spin is localized on one Fe site, it can experience the effect of the terminal ligand on the distal Fe. Thus the [2Fe-2S] core can be viewed as a single robust structural unit in its interaction with the terminal ligands, similar to the [4Fe-4S] core in the cubane complexes.[38,39]

4.3. [2Fe-2S] Complexes with Carboxylate Ligands: Influence of Coordination Geometries on the Electronic Structure. In our previous study on mixed-ligand cubane complexes,[39] we observed that the electron binding energies of the cubane complexes increase when SEt or Cl is substituted by a carboxylate ligand (OAc or OPr) because the carboxylate ligands are stronger electron acceptors than SEt or Cl. As discussed above and shown in Figure 5, the electron binding energies of the mixed-ligand [2Fe-2S] complexes also exhibit a linear relationship relative to the substitution number for the Cl/CN, SEt/CN, and SEt/Cl systems, similar to that observed in the cubane complexes. However, the PES spectra and binding energy trends of the [2Fe-2S] complexes with carboxylate ligands (Figure 2d,c) were very different from the cubane complexes with the same ligands: the substitution of either Cl or SEt by OAc or OPr decreases the electron binding energies. In the case of $[Fe_2S_2(OAc)_2]^-$ or $[Fe_2S_2(OPr)_2]^-$, even the spectral pattern changed significantly: the X and A features were no longer well-resolved. These observations suggested profound changes in the coordination environment of the carboxylate ligands in the [2Fe-2S] complexes.

In the cubane complexes, each Fe site is tetracoordinated and the carboxylate ligands act like monodentate ligands. Considering the high reactivity of the unsatisfied three-coordinate Fe sites and the potential for carboxylate to act as a bidentate ligand, we suspect that the dramatic differences observed in the PES spectra of the [2Fe-2S] complexes with carboxylate ligands must be due to the formation of a tetracoordinated iron site, as schematically shown in Figure 6b for $[Fe_2S_2Cl(OAc)]^-$. Thus, the coordination property of the carboxylate group changes and it acts as a bidentate ligand to satisfy the fourth coordination of the iron site in the [2Fe-2S] fission products. A four-membered ring is formed, despite the anticipated high strain. The decrease in electron binding energies suggests that the bidentate carboxylate ligands act more like electron donors, in contrast to the monodentate carboxylate ligands, which are more electron-withdrawing relative to SEt or Cl. The broad PES spectra of $[Fe_2S_2(OAc)_2]^-$ or $[Fe_2S_2(OPr)_2]^-$ (Figure 2d,e) indicate that either the carboxylate ligands change the electronic structure of the [2Fe-2S] core significantly or there might be two different isomers present. The PES spectra of the mixed-ligand complexes, $[Fe_2S_2Cl(OAc)]^-$ and $[Fe_2S_2(SEt)(OPr)]^-$, are not too different from those of the all-Cl or all-SEt complexes (Figure 2d,e), indicating that the carboxylate ligands do not perturb the electronic structure of the [2Fe-2S] core significantly and they can still be described by the inverted level scheme, as shown in Figure 6b. Thus we believe that the broad spectra of $[Fe_2S_2(OAc)_2]^-$ and $[Fe_2S_2(OPr)_2]^-$ were most likely due to the presence of two isomers, perhaps one with both the carboxylate ligands tetracoordinated and another with one tetra- and one tricoordinated carboxylate.

The electronic structure of the [2Fe-2S] clusters with one iron site tricoordinated and the other site tetracoordinated is interesting. In our previous investigations on [1Fe] complexes, $[Fe(SCH_3)_3]^-$ and $[Fe(SCH_3)_4]^-$, we showed that the ferrous center (Fe^{2+}) prefers tricoordination, whereas the ferric center (Fe^{3+}) prefers tetracoordination. Thus in the mixed-ligand [2Fe-2S] complexes with one terminal carboxylate ligand, the HOMO electron with a minority d spin state would localize on the Fe site that is not coordinated by the carboxylate, as shown in Figure 6b. This may also explain why there might be two isomers coexisting for $[Fe_2S_2(OAc)_2]^-$ or $[Fe_2S_2(OPr)_2]^-$, because a tri- or tetracoordination by the carboxylate ligand to the ferrous site in these complexes may be energetically competitive.

It is interesting to note that tetracoordination in the [2Fe-2S] complexes decreases its electron binding energies, that is, making the complexes better reductants. This may provide an explanation for a potential role of the newly discovered central atom in FeMoco.[52−56] Without the central atom, there are six "belt" ferrous Fe sites in FeMoco, which are essentially tricoordinated. The central atom would provide the fourth coordination, which would significantly enhance the reducing capability of the FeMoco and thus its catalytic function for nitrogen fixation. Whether this would be one of the functions of the central ligand deserves further investigation.

5. Conclusions

Photoelectron spectroscopy was used to investigate the electronic structures of five series of [2Fe-2S] complexes, $[Fe_2S_2Cl_{2-x}(CN)_x]^-$, $[Fe_2S_2(SEt)_{2-x}Cl_x]^-$, $[Fe_2S_2(SEt)_{2-x}(CN)_x]^-$, $[Fe_2S_2Cl_{2-x}(OAc)_x]^-$, and $[Fe_2S_2(SEt)_{2-x}(OPr)_x]^-$ ($x = 0-2$), which were generated by collision-induced dissociation of parent cubane complexes. The photoelectron spectra revealed that the electronic structure of these [2Fe-2S] species are similar to that of the cubane parents and can be described by the "inverted energy scheme". For the first three series that do not involve carboxylate ligands, it was shown that the electron binding energies increase with the substitution number linearly, suggesting that the terminal ligands contribute to the redox potentials of the [2Fe-2S] complexes independently and additively. The contribution of the different ligands to the electron binding energies was found to increase in the order SEt → Cl → CN, that is, proportional to the electron-withdrawing capability of the ligands. However, in the two series involving carboxylate ligands, the electron binding energies were observed to decrease with the substitution number. This was explained as due to the fact that the carboxylate ligands act as bidentate ligands in the [2Fe-2S] complexes, resulting in tetracoordinated Fe sites, even though they are known to behave as monodentate ligand in the cubane [4Fe-4S] complexes. The tetracoordination significantly decreases the electron binding energies of the [2Fe-2S] complexes, making them stronger reductants.

Acknowledgment. We thank Professors R. H. Holm's and Chris Pickett's groups for providing us initially the $[Fe_4S_4L_4]^{2-}$ precursor samples. Dr. Shuqiang Niu and Professor T. Ichiye are gratefully acknowledged for valuable discussions. This research was supported by the National Institutes of Health (GM-63555) and was performed at the Environmental Molecular Sciences Laboratory, a national scientific user facility sponsored by DOE's Office of Biological and Environmental Research and located at Pacific Northwest National Laboratory, which is operated for DOE by Battelle.

References and Notes

(1) Beinert, H.; Holm, R. H.; Munck, E. *Science* **1997**, *277*, 653.
(2) Holm, R. H.; Kennepohl, P.; Solomon, E. I. *Chem. Rev.* **1996**, *96*, 2239.
(3) Rao, P. V.; Holm, R. H. *Chem. Rev.* **2004**, *104*, 527.
(4) Kim, J.; Rees, D. C. *Science* **1992**, *257*, 1677.
(5) Kim, J.; Rees, D. C. *Nature* **1992**, *360*, 553.
(6) Chan, M. K.; Kim, J.; Rees, D. C. *Science* **1993**, *260*, 792.
(7) Einsle, O.; Tezcan, F. A.; Andrade, S. L. A.; Schmid, B.; Yoshida, M.; Howard, J. B.; Rees, D. C. *Science* **2002**, *297*, 1696.
(8) Barriere, F. *Coord. Chem. Rev.* **2003**, *236*, 71.
(9) Burgess, B. K.; Lowe, D. *J. Chem. Rev.* **1996**, *96*, 2983.
(10) Howard, J. B.; Rees, D. C. *Chem. Rev.* **1996**, *96*, 2965.
(11) Lee, S. C.; Holm, R. H. *Proc. Natl. Acad. Sci. U.S.A.* **2003**, *100*, 3595.
(12) Vela, J.; Stoian, S.; Flaschenriem, Munck, E.; Holland, P. L. *J. Am. Chem. Soc*. **2004**, *126*, 4522.
(13) Smith, J. M.; Lachicotte, R. J.; Pittard, K. A.; Cundari, T. R.; Lukat-Rodgers, G.; Rodgers, K. R.; Holland, P. L. *J. Am. Chem. Soc*. **2001**, *123*, 9222.
(14) Power, P. P.; Shoner, S. C. *Angew. Chem., Int. Ed*. **1991**, *30*, 330.
(15) MacDonnell, F. M.; Ruhlandt-Senge, K.; Ellison, J. J.; Holm, R. H.; Power, P. P. *Inorg. Chem.* **1995**, *34*, 1815.
(16) Sanakis, Y.; Power, P. P.; Stubna, A.; Munck, E. *Inorg. Chem.* **2002**, *41*, 2690.
(17) Calzolai, L.; Gorst, C. M.; Zhao, Z.-H.; Teng, Q.; Adams, M. W. W.; Mar, G. N. L. *Biochemistry* **1995**, *34*, 11373.
(18) Busse, S. C.; Mar, G. N. L.; Yu, L. P.; Howard, J. B.; Smith, E. T.; Zhao, Z.-H.; Adams, M. W. W. *Biochemistry* **1992**, *31*, 11952.
(19) Calzolai, L.; Gorst, C. M.; Bren, K. L.; Zhou, Z.-H.; Adams, M. W. W.; Mar, G. N. L. *J. Am. Chem. Soc*. **1997**, *119*, 9341.
(20) Yoo, S. J.; Angove, H. C.; Burgess, K. K.; Hendrich, M. P.; Munck, E. *J. Am. Chem. Soc*. **1999**, *121*, 2534.
(21) Angove, H. C.; Yoo, S. J.; Burgess, B. K.; Munck, E. *J. Am. Chem. Soc.* **1997**, *119*, 8730.
(22) Conover, R. C.; Park, J.-B.; Adams, M. W. W.; Johnson, M. K. *J. Am. Chem. Soc.* **1991**, *113*, 2799.
(23) Conover, R. C.; Kowal, A. T.; Fu, W.; Park, J.-B.; Aono, S.; Adams, M. W. W.; Johnson, M. K. *J. Biol. Chem.* **1990**, *265*, 8533.
(24) Telser, J.; Smith, E. T.; Adams, M. W. W.; Conover, R. C.; Johnson, M. K.; Hoffman, B. M. *J. Am. Chem. Soc.* **1995**, *117*, 5133.
(25) Jameson, G. N. L.; Walters, E. M.; Manieri, W.; Schurmann, P.; Johnson, M. K.; Huynh, B. H. *J. Am. Chem. Soc.* **2003**, *125*, 1146.
(26) Walsby, C. J.; Ortillo, D.; Broderick, W. E.; Broderick, J. B.; Hoffman, B. M. *J. Am. Chem. Soc.* **2002**, *124*, 11270.
(27) Clay, M. D.; Jenney, F. E.; Hagedoorn, P. L.; George, G. N.; Adams, M. W. W.; Johnson, M. K. *J. Am. Chem. Soc.* **2002**, *124*, 788.
(28) Telser, J.; Huang, H.; Lee, H.-I.; Adams, M. W. W.; Hoffman, B. M. *J. Am. Chem. Soc.* **1998**, *120*, 861.
(29) Noodleman, L.; Baerends, E. J. *J. Am. Chem. Soc*. **1984**, *106*, 2316.
(30) Li, J.; Nelson, M. R.; Peng, C. Y.; Bashford, D.; Noodleman, L. *J. Phys. Chem. A* **1998**, *102*, 6311.
(31) Norman, J. G., Jr.; Ryan, P. B.; Noodleman, L. *J. Am. Chem. Soc*. **1980**, *102*, 4279.
(32) Noodelman, L.; Norman, J. G., Jr.; Osborne, J. H.; Aizman, A.; Case, D. A. *J. Am. Chem. Soc*. **1985**, *107*, 3418.
(33) Zhai, H. J.; Kiran, B.; Wang, L. S. *J. Phys. Chem. A* **2003**, *107*, 2821.
(34) Yang, X.; Wang, X. B.; Fu, Y. J.; Wang, L. S. *J. Phys. Chem. A* **2003**, *107*, 1703.
(35) Yang, X.; Wang, X. B.; Wang, L. S.; Niu, S. Q.; Ichiye, T. *J. Chem. Phys*. **2003**, *119*, 8311.
(36) Niu, S. Q.; Wang, X. B.; Nichols, J. A.; Wang, L. S.; Ichiye, T. *J. Phys. Chem. A* **2003**, *107*, 2898.
(37) Wang, X. B.; Niu, S. Q.; Yang, X.; Ibrahim, S. K.; Pickett, C. J.; Ichiye, T.; Wang, L. S. *J. Am. Chem. Soc*. **2003**, *125*, 14072.
(38) Zhai, H. J.; Yang, X.; Fu, Y. J.; Wang, X. B.; Wang, L. S. *J. Am. Chem. Soc.* **2004**, *126*, 8413.
(39) Fu, Y. J.; Yang, X.; Wang, X. B.; Wang, L. S. *Inorg. Chem.* **2004**, *43*, 3647.
(40) (a) Yang, X.; Wang, X. B.; Niu, S. Q.; Pickett, C. J.; Ichiye, T.; Wang, L. S. *Phys. Rev. Lett.* **2002**, *89*, 163401. (b) Yang, X.; Wang, X. B.; Wang, L. S. *Int. J. Mass Spectrom.* **2003**, *228*, 797. (c) Niu, S. Q.; Wang, X. B.; Yang, X.; Wang, L. S.; Ichiye, T. *J. Phys. Chem. A* **2004**, *108*, 6750.
(41) Yang, X.; Niu, S. Q.; Ichiye, T.; Wang, L. S. *J. Am. Chem. Soc.* **2004**, *126*, 15790.
(42) Wang, L. S.; Ding, C. F.; Wang, X. B.; Barlow, S. E. *Rev. Sci. Instrum.* **1999**, *70*, 1957.
(43) Treichel, P. M.; Durren, G. E.; Mueh, H. J. *J. Organomet. Chem*. **1972**, *44*, 339.
(44) Pickett, C. J.; Pletcher, D. J. *J. Organomet. Chem*. **1975**, *102*, 327.
(45) Sarapu, A.; Fenske, R. F. *Inorg. Chem*. **1975**, *14*, 247.
(46) Lever, A. B. P. *Inorg. Chem*. **1990**, *29*, 1271.
(47) Wang, L. S.; Ding, C. F.; Wang, X. B.; Nicholas, J. B. *Phys. Rev. Lett.* **1998**, *81*, 2667.
(48) Wang, X. B.; Ding, C. F.; Wang, L. S. *Phys. Rev. Lett.* **1998**, *81*, 3351.
(49) Wang, X. B.; Wang, L. S. *Nature* **1999**, *400*, 245.
(50) Wang, L. S.; Wang, X. B. *J. Phys. Chem. A* **2000**, *104*, 1978.
(51) Wang, X. B.; Ding, C. F.; Wang, L. S. *Chem. Phys. Lett*. **1999**, *307*, 391.
(52) Kozak, C. M.; Mountford, P. *Angew. Chem., Int. Ed*. **2004**, *43*, 1186.
(53) Hinnemann, B.; Norskov, J. K. *J. Am. Chem. Soc*. **2004**, *126*, 3920.
(54) Dance, I. *Chem. Commun*. **2003**, 324.
(55) Schimpl, J.; Petrilli, H. M.; Blochl, P. E. *J. Am. Chem. Soc*. **2003**, *125*, 15772.
(56) Huniar, U.; Ahlrichs, R.; Coucouvanis, D. *J. Am. Chem. Soc*. **2004**, *126*, 2588.